Acta Crystallographica Section D
Biological Crystallography
ISSN 0907-4449

Purification, N-terminal sequencing, crystallization and preliminary structural determination of atratoxin-b, a short-chain α-neurotoxin from *Naja atra* venom

Xiaohua Lou,[a,b] Xiongying Tu,[a,b] Guoqiang Pan,[c] Chaoyin Xu,[c] Rong Fan,[c] Wanhua Lu,[d] Wenhan Deng,[d] Pingfan Rao,[d] Maikun Teng[a,b]* and Liwen Niu[a,b]*

[a]Key Laboratory of Structural Biology, Chinese Academy of Sciences, University of Science and Technology of China, 96 Jinzhai Road, Hefei, Anhui 230026, People's Republic of China, [b]Department of Molecular and Cell Biology, School of Life Sciences, University of Science and Technology of China, 96 Jinzhai Road, Hefei, Anhui 230026, People's Republic of China, [c]National Synchrotron Radiation Laboratory, University of Science and Technology of China, 96 Jinzhai Road, Hefei, Anhui 230026, People's Republic of China, and [d]Institute of Biotechnology, Fuzhou University, Fuzhou, Fujian 350002, People's Republic of China

Correspondence e-mail: lwniu@ustc.edu.cn

Received 5 September 2002
Accepted 11 March 2003

PDB Reference: atratoxin-b, 1onj, r1onjsf.

Atratoxin-b, a short-chain α-neurotoxin purified from *Naja atra* (mainland Chinese cobra) venom using a three-step chromatography procedure, has an apparent molecular mass of 6950 Da with an alkaline pI value (>9.5) and consists of one single polypeptide chain as estimated by MALDI–TOF mass spectrometry and SDS–PAGE. The protein is toxic to mice, with an *in vitro* LD_{50} of about 0.18 mg kg^{-1}. Its N-terminal amino-acid sequence, LECHN-QQSSQTPTIT, displays a very high homology to those of other α-neurotoxins. The overall three-dimensional structure of atratoxin-b is very similar to that of the homologous erabutoxin-a, as shown by the crystallographic molecular replacement and preliminary refinement results, with an R factor and R_{free} of 27 and 29%, respectively. The microcrystal slowly grew to dimensions of approximate 0.1 × 0.1 × 0.15 mm over eight months using hanging-drop vapour-diffusion method. It gave a set of diffraction data to 1.56 Å resolution using X-rays of wavelength 1.1516 Å generated by the X-ray Diffraction and Scattering Station of beamline U7B at the National Synchrotron Radiation Laboratory (Hefei, China); this is the first example of the use of this beamline in protein crystallography. The crystals belong to the tetragonal space group $P4_12_12$, with unit-cell parameters a = 49.28, c = 44.80 Å, corresponding to one molecule per asymmetric unit and a volume-to-mass ratio of 1.96 Å^3 Da^{-1}.

1. Introduction

The snake-venom α-neurotoxins from *Elapidae* and *Hydrophidae* venoms, consisting of 60–62 residues with four disulfide bridges, bind specifically to nicotinic acetylcholine receptors (nAChRs), blocking nerve transmission and leading to death from asphyxiation (Tu, 1973; Tsetlin, 1999; Juan *et al.*, 1999). All these short-chain proteins fold into a topological feature of three finger-like loops extending from a core region cross-linked by disulfide bonds and belong to a superfamily of three-finger proteins (Love & Stroud, 1986; Yu *et al.*, 1993). The essential role of the compactly conserved core is to stabilize the overall structure (Brown & Wuthrich, 1992; Hatanaka *et al.*, 1994), whereas the functional domain is observed as a non-conserved loop motif (Albrand *et al.*, 1995; Teixeira-Clerc *et al.*, 2002). The precise features of the loop regions may allow the functional residues in different neurotoxins to adopt a variety of arrangements with subtle differences and to recognize their specific targets (Ricciardi *et al.*, 2000). These properties are of use in basic medicine, serving as powerful tools for the investigation of the pharmacological and toxicological differences between various nAChRs (Endo & Tamiya, 1987; Changeux & Edelstein, 1998).

Although the high affinity and specificity of the binding of neurotoxins to their targets through a postulated mechanism of 'multi-attachment point character' are already known (Saez-Briones *et al.*, 1999; Martin *et al.*, 1983), the detailed structural features of functionally key residues are still unclear, partly because of a lack of available structural information for complexes of neurotoxins with their receptors. Structures of neurotoxins with different neuroactivities will help us to understand their functional similarities and differences.

The Protein Data Bank (PDB) contains more than ten structures of snake-venom short-chain α-neurotoxins determined by X-ray diffraction or two-dimensional NMR (Nastopoulos *et al.*, 1998; Low *et al.*, 1976; Corfield *et al.*, 1989; Saludjian *et al.*, 1992; Hatanaka *et al.*, 1994; ZinnJustin *et al.*, 1992; Yu *et al.*, 1993; Labhardt *et al.*, 1988). Crystal structures are only available of native and mutant forms from the *Hydrophidae* venom subclasses of α-neurotoxins; all the crystallized proteins belong to the space group $P2_12_12_1$ with slightly different unit-cell parameters and numbers of molecules in the asymmetric unit. They exhibit dimeric association through a parallel β-sheet around a twofold axis. The crystal structures of the cobra-venom subclass of α-neurotoxins are still unknown, although

their homologous structures in solution have been determined in a monomeric form.

We have previously reported the crystallization and preliminary diffraction analysis of atratoxin, an α-neurotoxin from *Naja atra* (mainland Chinese cobra) venom (Tu *et al.*, 2002); the amino-acid sequencing of atratoxin and its structural determination are in progress. Atratoxin-b, a highly homologous member of this family possessing an *in vitro* lethal activity that is noticeably different from that of atratoxin, has been purified from the same species and crystallized in a new crystal form. This paper describes the purification procedure, sequencing of the N-terminal amino-acid residues, crystallization and preliminary X-ray structural determination of this snake-venom protein.

2. Experimental procedures

2.1. Materials

Dried crude *N. atra* venom was obtained from the southern mountain region, Anhui Province, China. CM-Sepharose and Sephacryl S-100 were purchased from Pharmacia (Uppsala, Sweden). Standard protein markers were produced by Shanghai Institute of Biochemistry (Shanghai, China). Other chemicals and reagents were of analytical grade from commercial sources. Deionized water was used in the preparation of all solutions.

2.2. Protein purification and molecular characterization

The preparation of atratoxin-b was carried out by a three-step chromatography procedure at room temperature (about 298 K) (see Fig. 1). The purified samples were desalted and lyophilized for subsequent crystallization and characterization.

Both conventional SDS–PAGE and MALTI–TOF mass spectrometry were performed in order to check for homogeneity and to estimate the molecular weight.

The N-terminal amino-acid residue sequence was determined by the Edman degradation method as implemented on an Applied Biosystems 476A Protein sequencer located at Fuzhou University, China.

The lethal activity LD_{50} was assayed intravenously on laboratory mice according to the procedure of Aird & Kaiser (1985). Mice with body weights of 20–30 g were randomly assigned to five cages. Each cage contained five females and five males. Atratoxin-b was dissolved in phosphate-buffered saline (made by mixing 8.0 g NaCl, 0.2 g KCl, 0.2 g KH_2PO_4 and 0.15 g Na_2HPO_4 per litre and then adjusting the pH value to 7.1 with Na_2HPO_4) for injection. The *in vitro* injections were performed through one of two dorsolateral caudal veins. The outcome (survival or death) was recorded at 24 h post-injection. All operations were carried out at room temperature.

2.3. Crystallization and preliminary X-ray crystallographic analysis

The lyophilized protein was dissolved in double-distilled water and adjusted to a concentration of 15 mg ml^{-1}. The crystals were screened and grown at room temperature by the hanging-drop vapour-diffusion method using tissue-culture plates and siliconized glass cover slips. The Crystal Screen and Crystal Screen II kits (Hampton Research) were utilized to screen the initial crystallization conditions. Microcrystals could be seen after one week in drops made by mixing 2 µl of protein solution with 2 µl of precipitant solution (0.1 *M* Tris–HCl pH 8.5 containing 2.0 *M* ammonium sulfate), which then grew slowly to dimensions of approximately 0.1 × 0.1 × 0.15 mm (see Fig. 2) over eight months.

The diffraction data were recorded at room-temperature conditions from a single atratoxin-b crystal using a MAR 345 imaging plate (diameter 345 mm) mounted at the X-ray Diffraction and Scattering Station of beamline U7B, National Synchrotron Radiation Laboratory, Hefei, China. The wavelength was calibrated at 1.1516 Å by means of a least-squares refinement of silicon powder-diffraction rings using the program *FIT2D* (Hammersley, 2001). A total of 91 image frames were recorded at a crystal-to-detector distance of 150 mm (see Fig. 3). The oscillation angle was set to 1°. A dose-dependent exposure mode was chosen with a relative dose level of 8000. The data

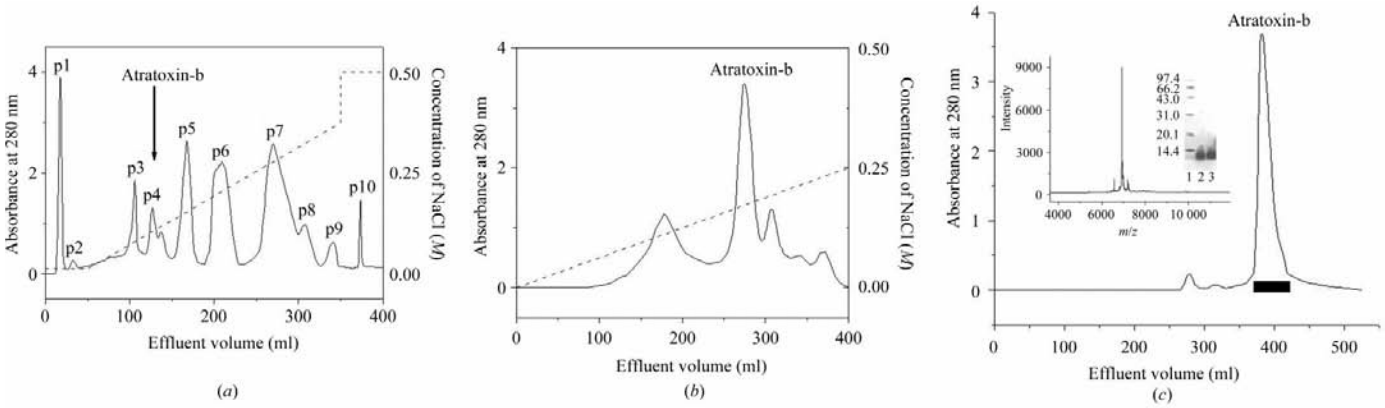

Figure 1
Purification of atratoxin-b from *N. atra* venom. (*a*) 0.5 g of dried crude venom was dissolved in 10 ml of buffer *A* (0.02 *M* $NaHPO_4/Na_2HPO_4$ pH 6.0), centrifuged at 10 000 rev min^{-1} to remove insoluble materials and then applied to a CM-Sepharose column (1 × 20 cm) pre-equilibrated with the same buffer. The elution was performed at a flow rate of 0.5 ml min^{-1} with a combined gradient of pH value and salt concentration produced by mixing 200 ml of buffer *A* with 200 ml of buffer *B* (0.02 *M* Na_2HPO_4/NaH_2PO_4 pH 8.0 containing 0.5 *M* NaCl) followed by two column volumes of buffer *B*. The fourth fraction, containing atratoxin-b, was pooled and desalted for further isolation. The absorbance at 280 nm is indicated by a solid line and the salt gradient by a dashed line. (*b*) The fraction from the previous column was applied to another CM-Sepharose column (1 × 20 cm) pre-equilibrated with buffer *A* and then eluted at a flow rate of 0.2 ml min^{-1} with a salt gradient made by mixing 200 ml of buffer *A* with 200 ml of buffer *C* (0.02 *M* $NaHPO_4/Na_2HPO_4$ pH 6.0 containing 0.5 *M* NaCl). The major fraction was pooled and concentrated for further gel filtration. (*c*) 2 ml of protein solution was loaded onto a Sephacryl S-100 column (2.6 × 80 cm) pre-equilibrated with 0.15 *M* NaCl solution and then eluted with the same solution at a flow rate of 0.5 ml min^{-1}. The component containing atratoxin-b (indicated by a solid bar) was pooled, desalted and lyophilized. Inset: the samples were transferred to a Bruker Biflex III MALDI–TOF mass spectrometer with a delayed extraction ion source equipped with a 337 nm nitrogen laser. The acceleration voltage was set to 20 kV. The pressure in the TOF analyzer was ~8×10^{-5} Pa. Sinapinic acid from Bruker was used as a matrix. Bovine insulin (5734 Da) and equine cytochrome *c* (12 360 Da) were used as an internal standard. The homogeneity was also demonstrated by SDS–PAGE: lane 2 and lane 3 are under reducing and non-reducing conditions, respectively; lane 1 contains protein standards with molecular weights in kDa.

were processed and reduced using *marFLM* (Bartels & Klein, 2000). The data-collection and reduction statistics are listed in Table 1.

The phase problem was solved by the molecular-replacement method using *AMoRe* (Navaza, 1994). The crystal structure of the homologous erabutoxin-a from *Laticauda semifasciata* venom (PDB code 5ebx) was chosen as a search model without any change in amino-acid residues, partly because the complete sequence of atratoxin-b has not yet been precisely determined. The rotation search was performed using an angular step size of 2.5° and a sphere radius of 30 Å within the resolution limits 15–3.5 Å. A translation search and rigid-body refinement gave a clear solution with a crystallographic R factor of 42.2%. The peak and noise correlation coefficients are 19 and 16.7%, respectively. Model rebuilding and preliminary refinement were carried out using the programs *CNS* (Brünger *et al.*, 1998) and *O* (Jones *et al.*, 1991). The crystallographic R factor and $R_{\rm free}$ decreased to 27 and 29%, respectively, after the necessary substitution of N-terminal amino-acid residues according to the determined sequence and several cycles of refinement of the diffraction data in the resolution range 20–1.56 Å, corresponding to a real-space R factor of 6.6% and a real-space correlation coefficient of 93.4%. The ambiguity in the crystallographic space group ($P4_12_12$ or $P4_32_12$) was resolved through structural refinement, in which the selection of $P4_32_12$ displayed non-convergence (experimental data not shown).

3. Results and discussion

A small snake-venom protein, atratoxin-b, has been purified from *N. atra* (mainland Chinese cobra) venom using a three-step chromatography procedure (Fig. 1). Atratoxin-b has an apparent molecular mass of 6950 Da with an alkaline pI value (>9.5) (experimental data not shown) and consists of one single polypeptide chain, as estimated by one sharp molecular-weight peak in a MALDI–TOF mass spectrum and one single band on an SDS–PAGE under both reducing and non-reducing conditions (see inset in Fig. 1*c*). The experimentally determined N-terminal amino-acid sequence of atratoxin-b, LECHNQQSSQTPTIT, displays a very high homology with those of other short-chain α-neurotoxins (Tu *et al.*, 2002; Yu *et al.*, 1993; Chang *et al.*, 1997; Strydom & Botes, 1971; Gregoire & Rochat, 1977; Chung *et al.*, 1994; ZinnJustin *et al.*, 1992; Corfield *et al.*, 1989; Low *et al.*, 1976; Fuse *et al.*, 1990). The overall three-dimensional structure of atratoxin-b is very similar to that of the homologous erabutoxin-a, as shown by the crystallographic molecular replacement and preliminary refinement results. Therefore, atratoxin-b should be classified as a new member of the short-chain α-neurotoxin family with a typical N-terminal sequence LECHNQQ and residue repetitions (*e.g.* QQ and SS). Atratoxin-b is toxic to mice with an *in vitro* LD_{50} of about 0.18 mg kg^{-1}. This lethal activity is weaker than that of the highly homologous atratoxin ($LD_{50} \simeq 0.08$ mg kg) previously purified from the same species (Tu *et al.*, 2002). The natural mutations (*e.g.* the two Thr residues at sites 8 and 9 are replaced by two Ser residues) and the notable difference in LD_{50} values might have structural or functional implications for their recognition by the related receptors.

There are significant differences between the crystallization conditions of atratoxin-b and atratoxin. It is not necessary to add any metal ions to the mother liquor when crystallizing atratoxin-b, while Cu^{2+} ions must be present during the growth of atratoxin crystals (Tu *et al.*, 2002). The crystallized atratoxin-b belongs to the tetragonal space group $P4_12_12$, with unit-cell parameters a = 49.28, c = 44.80 Å, corresponding to one molecule per asymmetric unit and a volume-to-mass ratio of 1.96 Å^3 Da^{-1} (Matthews, 1968). These crystallographic properties of atratoxin-b are different from those of the homologous atratoxin and erabutoxin-a; the latter two crystals belong to space groups $C222_1$ and $P2_12_12_1$, respectively.

Most of residues in the atratoxin-b structure display a good model fit to electron density after preliminarily refinement (Fig. 4). The overall structure of atratoxin-b shows a molecular topology that is very similar to that of short-chain α-neurotoxins as well as that of three-finger proteins (Fig. 5). There are eight molecules in the unit cell of atratoxin-b (Fig. 6). Similar to other known crystal structures of α-neurotoxins from *Laticauda semifasciata* venom (Nastopoulos *et al.*, 1998; Saludjian *et al.*, 1992), two molecules in adjacent asymmetric units could form a dimer through intermolecular association of two parallel three-stranded β-sheets (Fig. 5), although dimerization of atratoxin-b has not yet been detected in solution. Such dimerization may be a universal structural feature and is believed to be involved in the binding of short-chain α-neurotoxins to their receptors. The sequencing of all amino-acid residues and structural determination for atratoxin-b, as well as atratoxin, are being carried out in our laboratory, which will provide further insight into structural features of short-chain α-neurotoxins.

Attention should be paid to the X-ray source used in data collection from atratoxin-b crystals. Hard X-rays generated by synchrotron-radiation sources have become the conventional tool for structural analysis of biomacromolecular crystals. The National

Table 1
Statistics of data collection and reduction.

Values in parentheses are for the highest resolution shell (1.64–1.56 Å).

Space group	$P4_12_12$
Unit-cell parameters	
a (Å)	49.28
c (Å)	44.80
Resolution limits (Å)	16.57–1.56
Observations	87491
Independent reflections	8305
$R_{\rm merge}$†	0.082 (0.39)
Completeness‡ (%)	99.9 (99.9)

† $R_{\rm merge} = \sum_h \sum_j |I(h)_j - \langle I(h)\rangle| / \sum_h \sum_j I(h)_j$, where $I(h)_j$ is the observed intensity of the jth reflection and $\langle I(h)\rangle$ is the mean intensity of reflection h. ‡ Completeness is the ratio of the number of reflections to that of possible reflections.

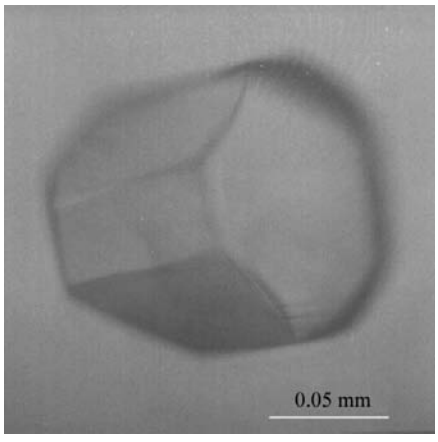

Figure 2
Photomicrograph of a crystal of atratoxin-b.

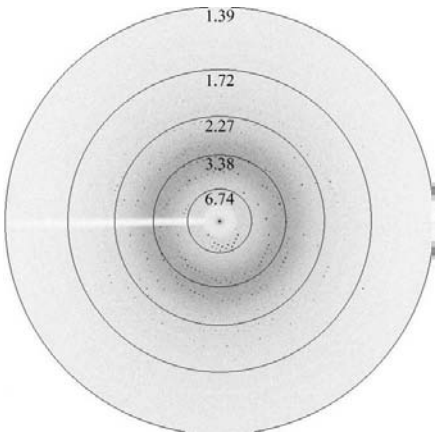

Figure 3
A diffraction pattern from an atratoxin-b crystal.

Synchrotron Radiation Laboratory (Hefei, China) has made progress recently in building a technical service system for protein crystallography to significantly support the efforts of structural biology and structural genomics in China. The X-ray diffraction of atratoxin-b reported here is the first example of the use of this service.

Financial support for this project to LN and MT was provided by research grants from the National Natural Science Foundation of China (Grant Nos. 39870108, 30025012, 39970175 and GG0854), the 973 and 863 Plans of the Ministry of Science and Technology of China (Grant Nos. G1999075603 and 2001AA233021) and the Chinese Academy of Sciences (Grant Nos. STZ-2-07, STZ98-2-12 and STZ01-29).

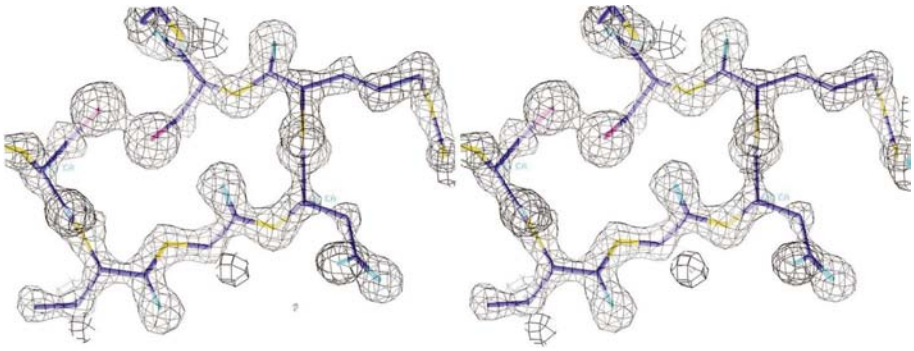

Figure 4
Amino-acid residues 55–61 superimposed on a $2F_o - F_c$ map (contoured at 2.0σ), showing the quality of the preliminarily refined structure of atratoxin-b. The figure was produced using the program *O*.

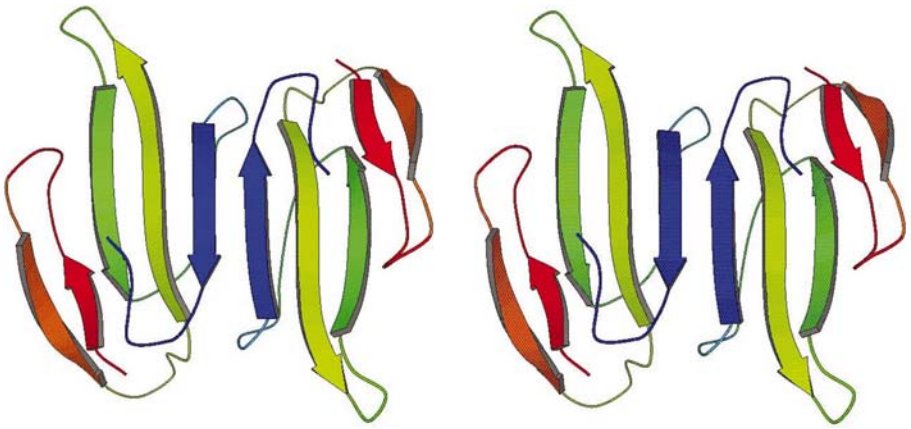

Figure 5
A dimer of atratoxin-b molecules related by a crystallographic twofold axis in crystals. The figure was produced using the program *O*.

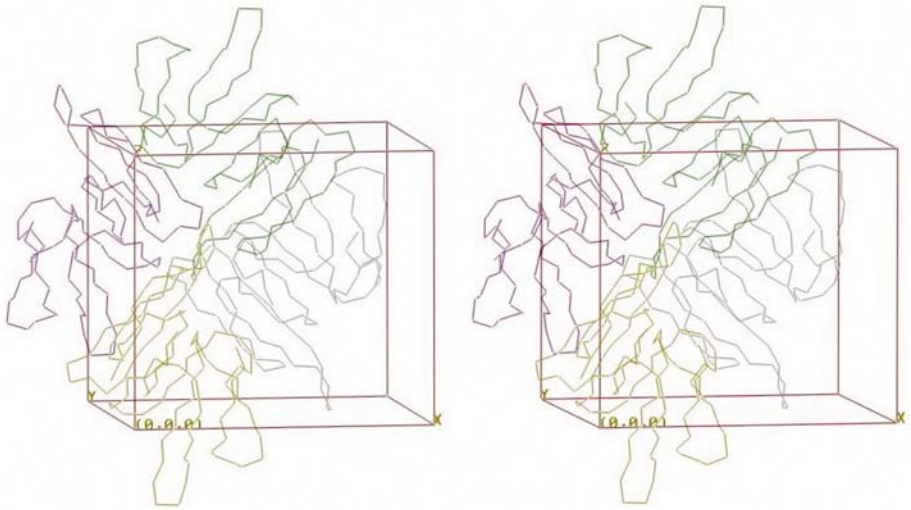

Figure 6
Close packing of atratoxin-b molecules in crystals. The figure was produced using the program *O*.

References

Aird, S. D. & Kaiser, I. I. (1985). *Toxicon*, **23**, 361–374.

Albrand, J. P., Blackledge, M. J., Pascaud, F., Hollecker, M. & Marion, D. (1995). *Biochemistry*, **34**, 5923–5937.

Bartels, K. & Klein, C. (2000). *MarFLM* version 5.0. X-ray Research GmbH, Segeberger Chaussee 34, D-22850 Norderstedt, Germany.

Brown, L. R. & Wuthrich, K. (1992). *J. Mol. Biol.* **227**, 1118–1135.

Brünger, A. T., Adams, P. D., Clore, G. M., DeLano, W. L., Gros, P., Grosse-Kunstleve, R. W., Jiang, J. S., Kuszewski, J., Nilges, M., Pannu, N. S., Read, R. J., Rice, L. M., Simonson, T. & Warren, G. L. (1998). *Acta Cryst.* D**54**, 905–921.

Chang, L. S., Chou, Y. C., Lin, S. R., Wu, B. N., Lin, J., Hong, E., Sun, Y. J. & Hsiao, C. D. (1997). *J. Biochem.* **122**, 1252–1259.

Changeux, J. P. & Edelstein, S. J. (1998). *Neuron*, **21**, 959–980.

Chung, M. C., Tan, N. H. & Argugam, A. (1994). *Toxicon*, **32**, 1471–1474.

Corfield, P. W., Lee, T. J. & Low, B. W. (1989). *J. Biol. Chem.* **264**, 9239–9242.

Endo, T. & Tamiya, N. (1987). *Pharmacol. Ther.* **34**, 403–451.

Fuse, N., Tsuchiya, T., Nonomura, Y., Menez, A. & Tamiya, T. (1990). *Eur. J. Biochem.* **193**, 629–633.

Gregoire, J. & Rochat, H. (1977). *Eur. J. Biochem.* **80**, 283–293.

Hammersley, A. (2001). *FIT2D*, version 10.132. ESRF, Grenoble, France.

Hatanaka, H., Oka, M., Kohda, D., Tate, S., Suda, A., Tamiya, N. & Inagaki, F. (1994). *J. Mol. Biol.* **240**, 155–166.

Jones, T. A., Zou, J. Y., Cowan, S. W. & Kjeldgaard, M. (1991). *Acta Cryst.* A**47**, 110–119.

Juan, H. F., Hung, C. C., Wang, K. T. & Chiou, S. H. (1999). *Biochem. Biophys. Res. Commun.* **257**, 500–510.

Labhardt, A. M., Hunziker-Kwik, E. H. & Wuthrich, K. (1988). *Eur. J. Biochem.* **177**, 295–305.

Love, R. A. & Stroud, R. M. (1986). *Protein Eng.* **1**, 37–46.

Low, B. W., Preston, H. S., Sato, A., Rosen, L. S., Searl, J. E., Rudko, A. D. & Richardson, J. S. (1976). *Proc. Natl Acad. Sci. USA*, **73**, 2991–2994.

Martin, B. M., Chibber, B. A. & Maelicke, A. (1983). *J. Biol. Chem.* **258**, 8714–8722.

Matthews, B. W. (1968). *J. Mol. Biol.* **33**, 491–497.

Nastopoulos, V., Kanellopoulos, P. N. & Tsernoglou, D. (1998). *Acta Cryst.* D**54**, 964–974.

Navaza, J. (1994). *Acta Cryst.* A**50**, 157–163.

Ricciardi, A., le Du, M. H., Khayati, M., Dajas, F., Boulain, J. C., Menez, A. & Ducancel, F. (2000). *J. Biol. Chem.* **275**, 18302–18310.

Saez-Briones, P., Krauss, M., Dreger, M., Herrmann, A., Tsetlin, V. I. & Hucho, F. (1999). *Eur. J. Biochem.* **265**, 902–910.
Saludjian, P., Prange, T., Navaza, J., Menez, R., Guilloteau, J. P., Ries-Kautt, M. & Ducruix, A. (1992). *Acta Cryst.* B**48**, 520–531.
Strydom, A. J. & Botes, D. P. (1971). *J. Biol. Chem.* **246**, 1341–1349.
Teixeira-Clerc, F., Menez, A. & Kessler, P. (2002). *J. Biol. Chem.* **277**, 25741–25747.
Tsetlin, V. (1999). *Eur. J. Biochem.* **264**, 281–286.
Tu, A. T. (1973). *Annu. Rev. Biochem.* **42**, 235–258.
Tu, X. Y., Huang, Q. Q., Lou, X. H., Teng, M. K. & Niu, L. W. (2002). *Acta Cryst.* D**58**, 839–842.
Yu, C., Bhaskaran, R., Chuang, L. & Yang, C. C. (1993). *Biochemistry*, **32**, 2131–2136.
ZinnJustin, S., Roumestand, C., Gilquin, B., Bontems, F., Menez, A. & Toma, F. (1992). *Biochemistry*, **31**, 11335–11347.